# **Inorganic Chemistry**

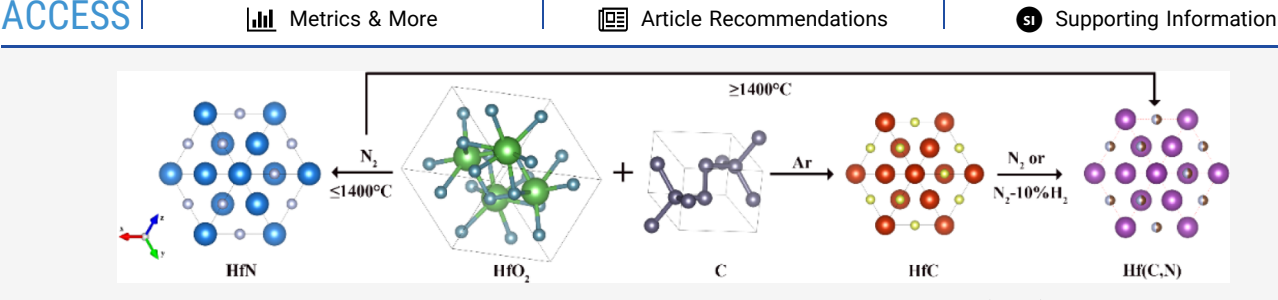
pubs.acs.org/IC Article

# Crystallographic Study of Product Phases of Carbothermic Reduction and Nitridation of Hafnium Dioxide

Chinthaka M. Silva,\* Kyle J. Kondrat, Kiel S. Holliday, and Scott J. McCormack







**ABSTRACT:** Details of the carbothermic reduction/nitridation to synthesize hafnium nitride (HfN) and hafnium carbide (HfC) are scarce in the literature. Therefore, this current study was carried out to evaluate two pathways for synthesizing these two refractory materials: direct nitridation and carbothermic reduction/nitridation. Two mixtures of hafnium dioxide and carbon with C/HfO<sub>2</sub> molar ratios of 2.15 and 3.1 were nitridized directly using flowing nitrogen gas at elevated temperatures (1300–1700 °C). The 3.1 C/HfO<sub>2</sub> molar ratio mixture was also carbothermically reduced under flowing argon gas to synthesize HfC, which was converted into HfN by introducing a nitridation step under both  $N_{2(g)}$  and  $N_{2(g)}$ -10%  $H_{2(g)}$ . X-ray diffraction results showed the formation of HfN at 1300 and 1400 °C and HfC<sub>1-y</sub>N<sub>y</sub> at  $\geq$ 1400 °C under direct nitridation of samples using a C/HfO<sub>2</sub> molar ratio of 2.15. These phase analysis data together with lower lattice strain and greater crystallite sizes of HfC<sub>1-y</sub>N<sub>y</sub> that formed at higher temperatures suggested that the HfC<sub>1-y</sub>N<sub>y</sub> phase is preferred over HfN at those temperatures. Carbothermic reduction of 3.1 C/HfO<sub>2</sub> molar ratio samples under an inert atmosphere produced single-phased HfC with no significant levels of dissolved oxygen. Carbothermic reduction nitridation made two phases of different carbon levels (HfC<sub>1-y</sub>N<sub>y</sub> and HfC<sub>1-y</sub>N<sub>y</sub>, where y' < y), while direct nitridation produced a single HfC<sub>1-y</sub>N<sub>y</sub> phase under both N<sub>2</sub> and N<sub>2</sub>-10% H<sub>2</sub> cover gas environments.

#### 1. INTRODUCTION

Hafnium nitride (HfN) is a refractory material that has favorable properties such as high reported melting point (3300-3387 °C),<sup>1,2</sup> high hardness, high elastic moduli,<sup>3</sup> low electrical resistivity ( $\sim$ 50  $\mu\Omega$  cm), good optical coating properties, high solar and infrared reflectivity, and high chemical stability against corrosion.<sup>6,7</sup> HfN is also a superconductor with transition temperatures  $(T_c)$  of 8.83 and 6.2 K.<sup>8–10</sup> It has been used as a coating layer in cemented carbide cutting tools to improve their performance and life due to its high hot hardness. 11 The favorable properties together with the bright metallic/gold color of HfN also lend it for use as coatings in turbine blades and window glasses not only as a decorating medium but also to improve product properties.<sup>12</sup> HfN is experimented in the field of plasmonic photothermal catalysis 13 and has shown to have better solar and infrared reflectivities than silver, making it a good candidate for solar mirror applications.<sup>5</sup> Thin films of HfN have shown improved microhardness in the presence of Kr<sup>+</sup> ion irradiation. <sup>14</sup> The high thermal stability of HfN makes it a good candidate in metal oxide semiconductor device applications. 15,16 Not only HfN but also hafnium carbonitride Hf(C, N) has shown improved mechanical properties leading to its use as a hard coating material.<sup>17</sup> It has also been predicted for HfC<sub>0.75</sub>N<sub>0.22</sub>

to have highest known melting temperature based on ab initio calculations.  $^{18,19}$  A similar composition (HfC $_{\!0.76}N_{\!0.24})$  of Hf(C, N) has shown great resistant to ablation (3000 °C) making it an interesting material for vehicles for space explorations.  $^{20}$ 

Several methods for synthesizing HfN are reported in the literature. Metal sheets of hafnium react with nitrogen over a 876-1034 °C temperature range under pressure with a reported activation energy of  $238.5 \pm 12.6 \text{ kJ/mol.}^{21}$  Metal hydriding—dehydriding followed by the metal nitridation at large-scale has also been reported. Another study reported the synthesis of HfN by nitriding the hydride. Carbothermic reduction followed by nitridation or carbothermic nitridation has been used in the synthesis of HfN as well. Another study reported the synthesis of HfN or Hf(C, N) using a high-energy ball milling method. A similar approach is reported in a different study where high-energy ball milling was used to

Received: April 24, 2023 Published: July 17, 2023





synthesize fine HfN powder using hafnium metal with improved reaction kinetics.<sup>25</sup> Synthesis of Hf(C, N) at temperatures >1700 °C using reactive spark plasma sintering of mixtures of HfN and hafnium carbide (HfC) precursors is reported.<sup>26</sup> Hafnium metal was also nitridized to make HfN at moderate temperatures such as 600-1200 °C under N<sub>2</sub> and NH<sub>3</sub> gases with activation energies of 95.0 and 57.3 kJ/mol, respectively, suggesting N<sub>2</sub> gas to be more kinetically favorable. A full nitridation of hafnium using a mechanically activated partially hydrated HfCl<sub>4</sub>-Mg powder mixture was reported to form HfN free from oxide impurities.<sup>28</sup> In another study, a magnesium thermal reduction process in an autoclave was used to synthesize HfN at a considerably low temperature (1000 °C).<sup>29</sup> Selective laser melting or reaction has also been used in exploring novel routes to accommodate additive manufacturing efforts of HfN and HfC.<sup>30</sup> Techniques such as chemical vapor deposition, <sup>16</sup> physical vapor deposition, <sup>15</sup> activated reactive evaporation, <sup>11</sup> and DC magnetron sputtering, in which a lower electrical resistivity (20  $\mu\Omega$  cm) was reported for as-deposited HfN on SiO<sub>2</sub>, <sup>31</sup> have been used to coat HfN. N2+ ion implantation is also another way to synthesize HfN films.<sup>32</sup> Plasma spraying is also reported to be successful in coating HfN with improved nanomechanical properties.33

Even though these above-mentioned techniques have been used in synthesizing HfN and HfC for different applications and discussed in detail, carbothermic reduction/nitridation as a common method has not been conversed thoroughly in the literature. Therefore, the focus of this current study has been the systematic synthesis of HfN and HfC using the carbothermic reduction/nitridation of a mixture of hafnium oxide (HfO<sub>2</sub>) and carbon. Two precursor mixtures with C/ HfO<sub>2</sub> molar ratios of 2.15 and 3.1 were used in producing HfN using direct nitridation and carbothermic reduction/nitridation, respectively. The respective reactions involved in these two routes will be discussed in Sections 2.1 and 2.2. As a part of understanding the reaction associated in the carbothermic nitridation, direct nitridation was also used for samples consisting of 3.1 C/HfO<sub>2</sub>. As powder X-ray diffraction (XRD) is normally used to check the product phase purity and stoichiometry of these materials based on refined lattice parameter (LP) versus carbon level correlation plots, this study used XRD as the sole characterization technique.

#### 2. EXPERIMENTAL CONDITIONS

**2.1. Materials and Furnace.** Carbon nanopowder (particle size <100 nm) and hafnium oxide (HfO<sub>2</sub>: purity at 98%) were purchased from Sigma-Aldrich, USA. The feed stock powder mixture of carbon and HfO<sub>2</sub> was prepared using two different C/HfO<sub>2</sub> molar ratios (2.15 and 3.1), which is discussed in Sections 2.2 and 2.3. The two materials were hand ground and mixed using a mortar and pestle (Coors porcelain) for 30 min. 0.2–1 g of the feed stock material was used in the synthesis of carbide and nitride samples. A pre-backed cylindrical graphite crucible (45 mm internal diameter and 110 mm length) was used to hold the samples in the furnace during heat treatments. A MTI2000 (MTI Corporation, USA) induction furnace equipped with graphite and alumina insulations was used for the carbothermic reduction and nitridation processes in this study.

**2.2. Carbothermic Reduction of HfO<sub>2</sub>.** HfC can be synthesized by heat treating a mixture of carbon and HfO<sub>2</sub> under an inert atmosphere. According to stoichiometry in eq 1, a C/HfO<sub>2</sub> molar ratio of 3.0 is needed for this synthesis. However, Sacks et al. showed that a C/HfO<sub>2</sub> molar ratio of 3.1 is needed to observe the complete conversion of the oxide into the carbide as some of the carbon could be lost during handling and precursor preparation.<sup>34</sup> Therefore, the

current study also used a C/HfO $_2$  molar ratio 3.1 in synthesizing HfC. They also reported that >1600 °C temperature is optimal for the synthesis of HfC without dissolved oxygen. Therefore, a 1650–1750 °C temperature range was utilized here.

$$HfO_2 + 3C \rightarrow HfC + 2CO$$
 (1)

The HfO<sub>2</sub> with correct amount of nano carbon powder (C/HfO<sub>2</sub> molar ratio of 3.1) was mixed and grinded three times using a mortar and pestle (Coors porcelain) inside a fume hood for >30 min. Samples weighing ~0.4-1.0 g were used in a cylindrical graphite crucible (45 mm internal diameter and 110 mm height), which was inserted into the induction furnace. Samples heat treatments were performed at three different temperatures (1650, 1700, and 1750 °C) for up to 4 h under flowing ultra-high purity argon gas, which was gettered at 500 °C using copper powder (99.9% purity by Alfa Aesar, -100 + 325 mesh) prior to its introduction into the reaction chamber of the induction furnace. A large-scale (~8 g) sample was also carbothermically reduced at 1650 °C under Ar cover gas using a reaction time of 8 h at that temperature to synthesize HfC. The furnace chamber was evacuated (<10<sup>-1</sup> Torr pressure), followed by Ar purging for three times before starting furnace ramping. Both ramping and cooling were carried out at a 27 °C/min rate. The cover gas flow was done at a rate of 150-200 cm<sup>3</sup>/min.

**2.3. Nitridation Reaction.** As depicted by eqs 2 and 3, the direct nitridation of HfO2 using C/HfO2 molar ratio of 2.0 and the nitridation of HfC should form HfN. Therefore, two different routes were explored to synthesis HfN in this study. That is, the direct nitridation of a mixture of HfO2 and carbon at C/HfO2 molar ratios of 2.15 and 3.1 and the carbothermic reduction followed by nitridation of a mixture of C/HfO2 at 3.1 molar ratio. In the first route, nitridation was conducted under N2 (UHP grade) with one sample under N2-10% H2 (UHP grade) to check any differences in the product phase. In the second route, carbothermic reduction of the oxide and carbon mixture was conducted under Ar followed by nitridation under N2-10% H2. Since the first step of this route involves the synthesis of HfC, the nitridation step is actually similar to the nitridation of HfC. The nitridation reaction of the second route was also performed under N<sub>2</sub> to help understand the nitridation reaction and its product phase characteristics. Note that C/HfO2 molar ratios of 2.15 and 3.1 precursor compositions will be designated as HfO<sub>2</sub>-2.15C and HfO<sub>2</sub>-3.1C, respectively, from this point onward.

As in the HfC synthesis, a cylindrical graphite crucible of similar size was used to hold the samples weighing  $\sim\!0.3-1.0$  g. Furnace chamber evacuation-purging, its ramping and cooling, and cover gas flow rates were similar to that of the carbothermic reduction reaction mentioned in Section 2.2. Nitridation of HfO2-2.15C samples under  $N_2$  cover gas was performed at 1300, 1400, 1500, 1650, and 1700 °C temperatures with 4–12 h reaction time. A few large-scale samples (5 g) of HfO2-2.15C were also nitridized under  $N_2$  at 1650 °C with up to 24 h reaction time. Carbothermic reduction of HfO2-3.1C samples under Ar cover gas and both under  $N_2$ -10%  $H_2$  and  $N_2$  cover gases were carried out at only 1650 °C based on the results acquired from the earlier experiments performed here.

$$HfO_2 + 2C + 1/2N_2 \rightarrow HfN + 2CO$$
 (2)

$$HfC + 3/2N_2 + H_2 \rightarrow HfN + 2HCN$$
 (3)

Note that HCN is a toxic gas, and our experiments were conducted using small scale sample sizes and the downstream cover gas was flown to a water bubbler in which any evolved HCN gas was neutralized.

**2.4. X-ray Diffraction.** Sample characterization was performed using a D8 Discover (Bruker Inc.) powder X-ray diffractometer equipped with Cu  $K_{\alpha}$  radiation. Powder XRD patterns were collected in a  $10-120^{\circ}$  2Theta range using  $0.01-0.005^{\circ}$  step size with 0.325 s/step over a total of 2 h scanning time. General structure analysis system software was used to perform the XRD pattern fitting using the Rietveld refinement. Either LaB<sub>6</sub>-660c or Si-640f NIST (National Institute of Standards and Technology) standards were also addmixed with the samples when collecting the XRD patterns.

Table 1. XRD Data of HfN Samples Synthesized Using HfO<sub>2</sub>-2.15C Precursor for 12 h at Different Reaction Temperatures<sup>a</sup>

		weight percentage (%)			LP (nm)		
sample	T (°C)	HfN Hf(C, N)	$Hf_7O_8N_4$ $Hf_2ON_2$	impurity phase	HfN Hf(C, N)	$Hf_7O_8N_4$	$Hf_2ON_2$
HfN-1	1300	41.5(3)	0.0	С	0.45088(1)	N/A	1.00588(1)
		45.4(4)	13.1(2)		0.45417(1)		
HfN-2	1400	5.9(4)	<3.0	С	0.45116(1)	0.94811(6)	1.00630(17)
		90.8(3)	<0.5		0.45716(1)	0.87837(9)	
HfN-3	1500	0	N/A	C, HfO <sub>2</sub>	N/A	N/A	N/A
		99.7(6)			0.45818(1)		
HfN-4	1650	0	N/A	C, HfO <sub>2</sub>	N/A	N/A	N/A
		>99			0.46012(1)		
HfN-5	1700	0	N/A	C, HfO <sub>2</sub>	N/A	N/A	N/A
		>99			0.46019(1)		
HfN-6	1650	0	N/A	$HfO_2$	N/A	N/A	N/A
		>99			0.45997(1)		
HfN-7	1650	0	N/A	$HfO_2$	N/A	N/A	N/A
		>99			0.45978(1)		

<sup>&</sup>lt;sup>a</sup>The second nitride phase in the 1300 °C (HfN-1) sample can also be a  $HfN_{1-x}O_x$ -type phase. The two 5 g large-scale samples (HfN-6 and -7) were synthesized at 1650 °C for 24 h. Graphite impurity in samples was from the crucible debris.

#### 3. RESULTS

# 3.1. Direct Nitridation of HfO<sub>2</sub>-2.15C Precursor.

Preliminary phase identification of the products in sample HfN-1 (Table 1) acquired by nitriding a HfO<sub>2</sub>-2.15C precursor sample at 1300 °C for 12 h indicated the presence of facecentered cubic (fcc) HfN and body-centered cubic Hf<sub>2</sub>ON<sub>2</sub> phases.<sup>36</sup> The refined LP) of the nitride phase of this sample [0.45088(1) nm] is comparable with the LPs of  $0.450^{21}$  and 0.4514 nm,<sup>27</sup> which is within the range of LPs of 0.449–0.450 nm obtained for an oxygen-free HfN as reported by Barraud et al. 28 This is also within the LP values reported in inorganic crystal structure database (ICSD) for HfN (Table S1: 0.45101-0.45500 nm). The presence of a second nitride phase was also identified during the profile fitting of this XRD pattern (Figure 1a,b) using Rietveld refinement. The peaks corresponding to this second phase were adjacent to that of the HfN phase and are to the lower 2Theta side, indicating the second phase to have a greater LP than the LP of HfN (Table 1). These peaks could be from a second nitride phase with either oxygen or carbon dissolved in it (Figure 1b), resulting in a composition of  $HfN_{1-x}O_x/or\ Hf(O, N)$  or  $HfC_{1-y}N_y/or$ Hf(C, N), respectively, as both oxygen and carbon increase the LP of the HfN phase (Tables S1-S2). However, the refined LP of this second phase [0.45417(1) nm] is closer to the range of LPs reported for the Hf(O, N) phase than that of the Hf(C, N) phase, indicating this second nitride phase to be derived from  $HfN_{1-x}O_x$  type composition. A minor peak at ~26.5° 2Theta was identified as graphite, which did not have sufficient intensity for peak fitting. It was later found that the graphite impurities came from the graphite crucible debris. XRD profile fitting showed 41.5(3) and 45.4(4) wt % of HfN and Hf(O, N), respectively, while the rest of the sample contained the 13.1(2) wt % Hf<sub>2</sub>ON<sub>2</sub> phase.

In sample HfN-2, heat treated at 1400 °C, the amount of HfN phase content decreased to 5.9(4) wt % and the second phase increasing up to a 90.8(3) wt %. The refined LP of HfN [0.45116(1) nm] of this sample also lies within the values reported for HfN, while the LP of the second phase 0.45716(1) nm matches with the reported LPs of the Hf(C, N) phase (Table S2). A  $Hf_7N_4O_8$  trigonal crystal phase isomorphous to  $Zr_7N_4O_8$  with the  $R\overline{3}H$  space group was also

identified in this sample.<sup>37</sup> The profile fitting of the XRD pattern indicated only <3.0 and <0.5 wt % of  $Hf_7N_4O_8$  and  $Hf_2ON_2$  ( $I\overline{a}$  space group) phases in the sample, respectively. These phases are depicted in profile-fitted plots shown in Figure 1c,d. Impurity peak of graphite that came from crucible debris is observed also in this sample.

Sample HfN-3, synthesized at 1500 °C only contained Hf(C, N) phase with a minor fcc- $HfO_2$  impurity phase usually present at <0.5 wt % due to surface oxidation under ambient conditions. Similar results obtained for samples synthesized at 1650 and 1700 °C. The profile-fitted XRD patterns of 1500 and 1650 °C samples are also shown in Figure 1e,f, respectively. A greater residual between the experimental and calculated XRD patterns can be observed in the profile fitted figures in the samples where two nitride phases present (Figure 1a–d) than in the single-phase nitride samples (Figure 1e,f), especially the samples synthesized at  $\geq$ 1650 °C (Figure 1f). This is because these samples have stacking faults at atomic scale that result in greater lattice strain as will be discussed further in the discussion section.

# 3.2. Carbothermic Reduction of HfO<sub>2</sub>-3.1C Precursor. Carbothermic reduction of the HfO<sub>2</sub>-3.1C sample carried out at 1650 °C under flowing Ar cover gas showed the presence of fcc-HfC as the primary phase as depicted in the XRD pattern in Figure S1 (sample HfC-1 in Table 2). The sample consisted of minor peaks corresponding to fcc-HfO2 secondary phase. Full profile fit carried out on the powder XRD pattern using the Rietveld analysis showed that this HfO2 phase is minor at <0.3 wt %. In order to check if this minor oxide phase forms as a result of incomplete carbothermic reduction reaction of the HfO<sub>2</sub>-3.1C precursor material, two other samples (HfC-2 and HfC-3) were synthesized at higher reaction temperatures of 1700 and 1750 °C under flowing Ar cover gas with the similar reaction time (4 h). The powder XRD patterns of these two samples also showed the presence of that minor HfO2 phase. The XRD patterns of all three samples synthesized at 1650, 1700, and 1750 °C are shown in Figure 2. As depicted in Table 2, the Rietveld analysis of these two samples also showed <0.3 wt % oxide phase. These two observations suggest that the HfO2 impurity phase formed during sample handling under ambient conditions and not as a result of incomplete HfO<sub>2</sub>-3.1C transformation into the carbide.

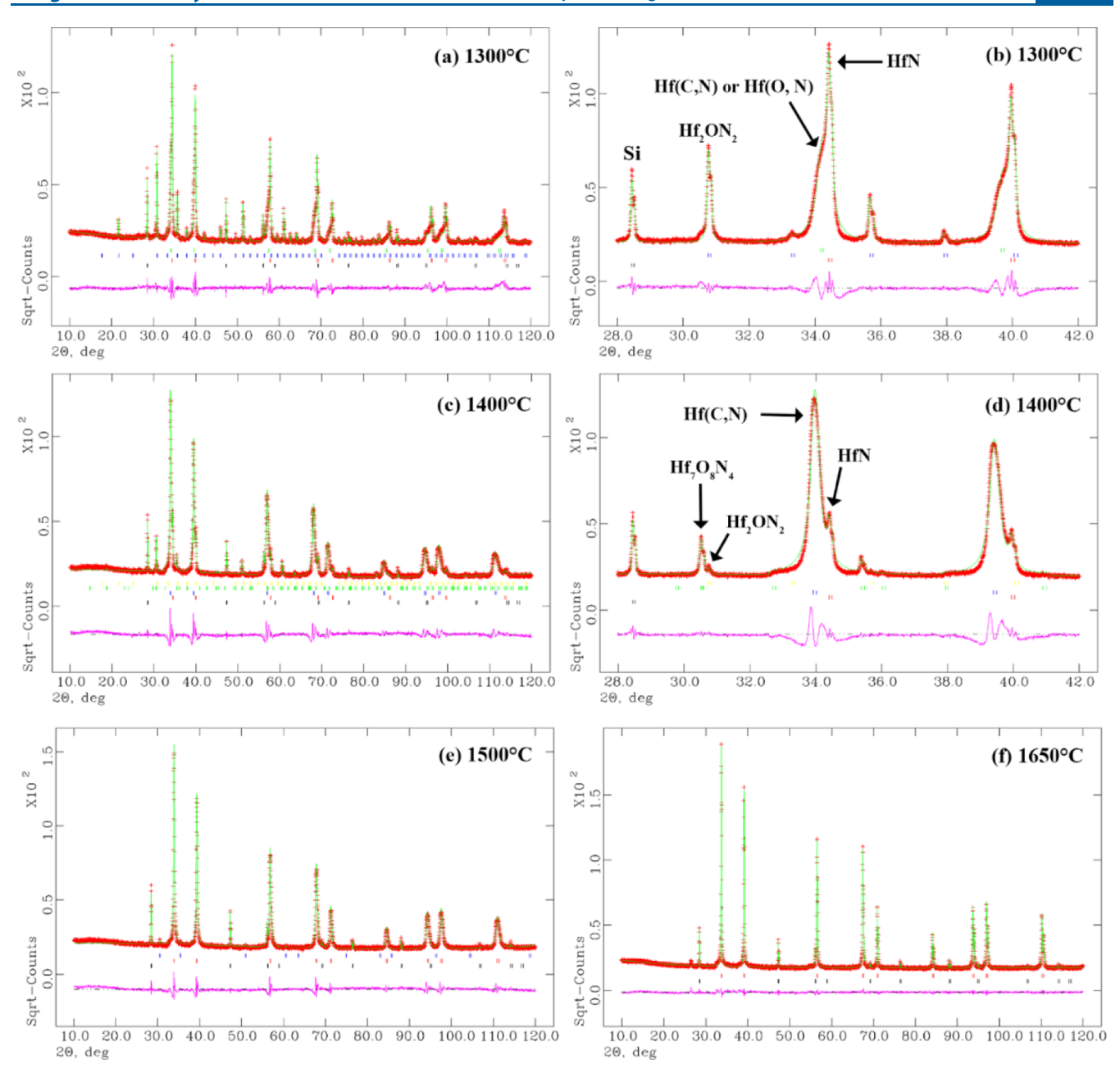


Figure 1. XRD patterns of HfN samples synthesized using the HfO<sub>2</sub>-2.15C precursor at different temperatures under  $N_2$  cover gas with a 12 h reaction time: (a,b) 1300, (c,d) 1400, (e) 1500, and (f) 1650 °C. Red, green, and pink color patterns correspond to the experimental, calculated, and the difference patterns, respectively. Impurity peak from graphite (at ~26.5° 2Theta) from the crucible debris is observed (e.g., in the 1650 °C).

The refined LPs of the synthesized HfC samples are listed in Table 2. The ICSD crystallography database reports a few HfC<sub>x</sub> (where  $0.9 \le x \le 1$ ) and HfC<sub>1-a</sub>O<sub>a</sub> compositions with the same fcc crystal structure. The reported LP for a starquality HfC is  $0.463078 \pm 0.00004$  nm (ICSD #159873),<sup>38</sup> while LPs of 0.4638, 0.4648, and  $0.46393 \pm 0.00005$  nm are also reported for HfC<sub>0.901</sub> (ICSD # 43371),<sup>39</sup> HfC<sub>0.95</sub> (ICSD #618007),<sup>40</sup> and HfC<sub>0.96</sub> (ICSD #617997)<sup>41</sup> compositions, respectively. A linear fit with a  $R^2$  value of 0.78 was obtained for the LPs of HfC<sub>0.95</sub>, HfC<sub>0.96</sub>, and HfC compositions (Figure S2). Assuming this linear variation corresponding to a linear fit of Y = -0.03069x + 0.4937, the C/Hf molar ratios of the three samples synthesized here were estimated to be  $\ge 0.98$ . Since the LPs of the reported HfC<sub>1-a</sub>O<sub>a</sub> compositions are in the

0.4603–0.4618 Å (ICSD # 196638 and 196637)<sup>42</sup> range, it was concluded that the oxygen dissolved in the synthesized HfC samples in the current study are insignificant.

The refined LPs (Table 2) of the secondary fcc-HfO<sub>2</sub> phase of the samples are within the reported value of  $0.5125 \pm 0.0010$  Å (ICSD # 53033).<sup>43</sup> Therefore, it can be concluded that the amount of carbon dissolved in the secondary HfO<sub>2</sub> phase in the samples are insignificant, suggesting the oxide phase formation to be on the HfC particle surfaces due to the sample handling under ambient conditions. As mentioned in Table 2, a carbide sample (HfC-4) was also synthesized at 1750 °C with only a 30 min of holding time. This sample also showed the presence of HfC with <0.3 wt % HfO<sub>2</sub> secondary

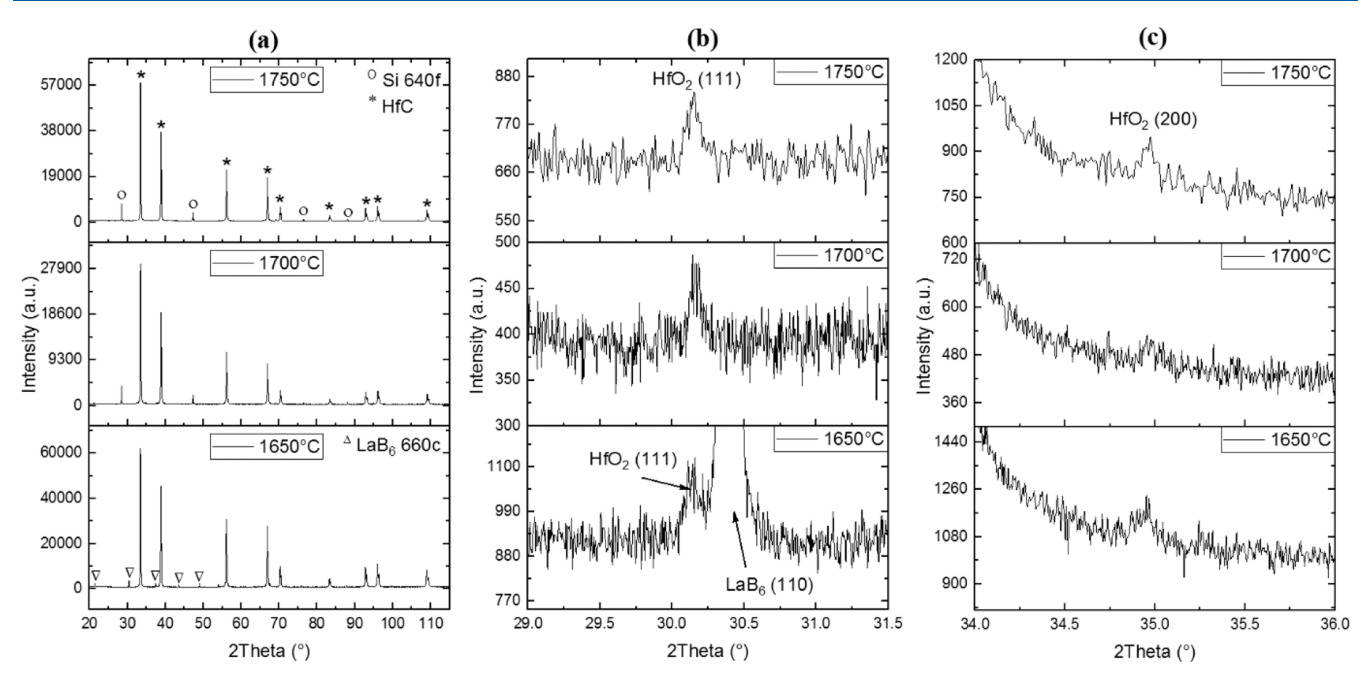


Figure 2. XRD patterns of HfC samples synthesized at 1650, 1700, and 1750  $^{\circ}$ C. The full XRD patterns and the enlarged regions highlighting (111) and (200) reflections of HfO<sub>2</sub> in figures (a–c), respectively.

Table 2. Experimental Conditions (4 h Reaction Time at Each Temperature) and the XRD Data of the Synthesized HfC Samples<sup>a</sup>

		wt	(%)	LP (nm)		
sample	synthesis temp. (°C)	HfC	HfO <sub>2</sub>	HfC	HfO <sub>2</sub>	estimated C/Hf molar ratio in HfC
HfC-1	1650	99.7	< 0.3	0.46368(1)	0.51325(9)	0.98
HfC-2	1700	99.8	< 0.2	0.46328(1)	0.51253(5)	0.99
HfC-3	1750	99.7	< 0.3	0.46349(1)	0.51280(8)	0.98
HfC-4	1750	99.7	< 0.3	0.46318(1)	0.51278(4)	0.99
HfC-5	1650	99.8	< 0.2	0.46343(1)	0.51289(4)	0.99

<sup>&</sup>lt;sup>a</sup>Only 30 min reaction time was used for the HfC-4 sample. Error values are shown in brackets.

Table 3. XRD Data of HfN Samples Synthesized Using HfO<sub>2</sub>-3.1C Precursor at 1650 °C<sup>a</sup>

			wt (%)		LP (nm)	
	sample	time under Ar and $N_2$ or $N_2\mbox{-}10\%~H_2$	$HfC_{1-y}N_y$	$HfC_{1-y'}N_{y'}$	$HfC_{1-y}N_y$	$HfC_{1-y'}N_{y'}$
090221	HfCN-1	0, 4	100	N/A	0.45982(1)	N/A
082321	HfCN-2	1, 4	87.492)	12.6(8)	0.46054(1)	0.46143(1)
081821	HfCN-3	2, 4	88.8(1)	11.2(9)	0.46093(1)	0.46177(1)
111021	HfCN-4	0, 4 <sup>H2</sup>	100	N/A	0.45990(1)	N/A
102021	HfCN-5	2, 4 <sup>H2</sup>	88.1(2)	11.6(7)	0.46049(1)	0.46125(1)

<sup>&</sup>quot;T, Ar,  $N_2$ " denote reaction time and Ar and  $N_2$  cover gases, respectively. " $H_2$ " indicates in the samples where  $N_2$ -10%  $H_2$  was used. Note that y' < y in the  $HfC_{1-y}N_y$  and  $HfC_{1-y'}N_{y'}$ .

phase. The LP of the sample was lowest with estimated C/Hf stoichiometry ratio of 0.99.

**3.3. Nitridation of HfO**<sub>2</sub>**-3.1C Precursor.** Direct nitridation of the HfO<sub>2</sub>-3.1C precursor for 4 h (sample HfCN-1 in Table 3) at 1650 °C produced a single phase with no significant residual in the profile fit of its XRD pattern to show the presence of a second phase (Figure S3a,b). However, the profile fits of the XRD patterns of samples HfCN-2 and HfCN-3 synthesized by carbothermic reduction, followed by nitridation showed the presence of two chemical phases (Figure S3c,d) and an example of peak fitting using single and two phases is shown in Figure S4. As shown in Figure 3, a peak shift to the low-angle side was observed in the samples

nitridized following a carbothermic reduction. The comparison in that figure also shows that the peak shift increases, which is confirmed by the increase in the refined LPs of the phases (Table 3), as the time used in the carbothermic reduction step (heat treatment under Ar) increases.

These LPs are also larger than the LPs observed for the HfNs (Table 1) and smaller than that of HfCs (Table 2). As verified in Section 3.2, carbothermic reduction of  $\rm ZrO_2$ -3.1C precursor produced HfC with no significantly dissolved oxygen in it. Therefore, it can be suggested that larger LPs of the phases in these samples are due to the formation of  $\rm HfC_{1-y}N_y$  type chemical phases. Since the LPs of the second phases fitted in the XRD patterns of these samples synthesized using two

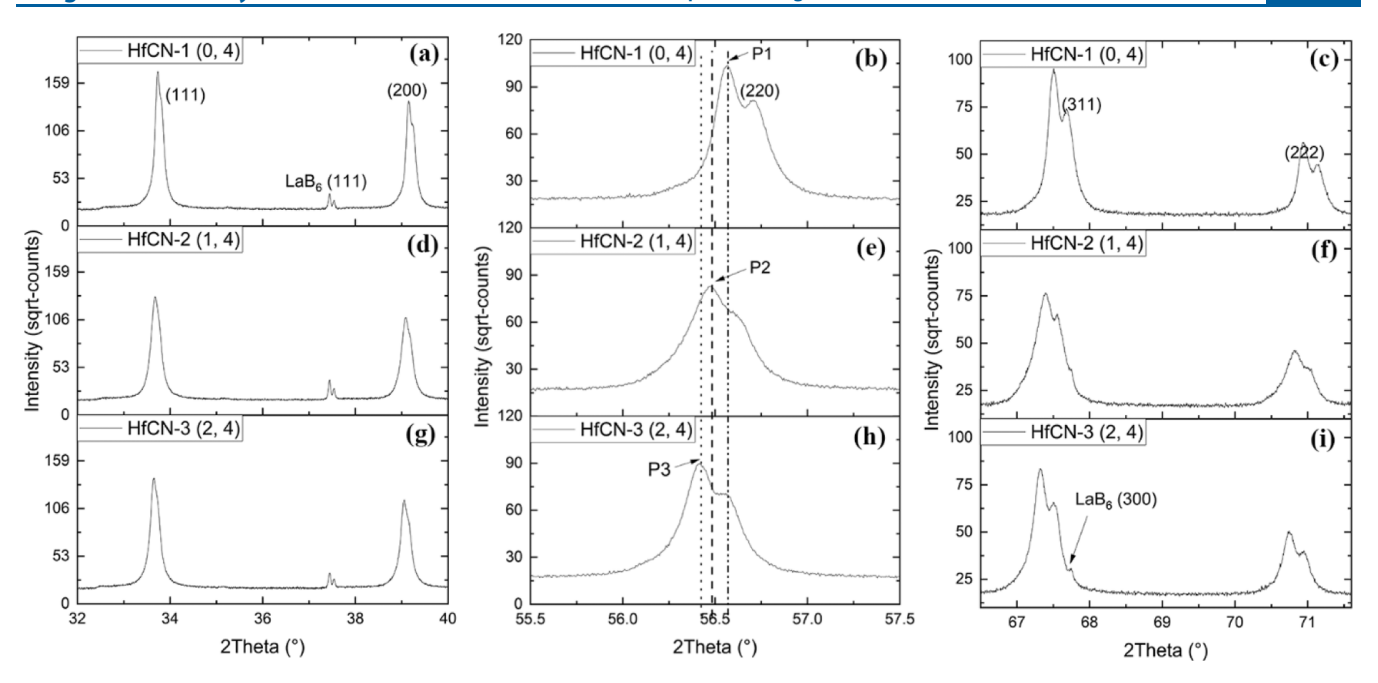


Figure 3. Comparison of a few peaks of HfN/HfC reflections in the nitride samples synthesized at 1650  $^{\circ}$ C using three different experimental conditions: the two digits in brackets of the sample names indicate the holding times under  $Ar_{(g)}$  and  $N_{2(g)}$ , e.g., HfCN-1 (0, 4) was held under Ar for 0 h and under  $N_2$  for 4 h.

steps are greater than that of the primary phase, a second chemical composition of  $HfC_{1-y'}N_{y'}$  can be suggested for that second phase, where y' < y. Samples synthesized using carbothermic reduction followed by nitridation using  $N_2$ -10%  $H_2$  also showed similar behavior, indicating that the effect of using reducing conditions was not significant on the product phases (samples HfCN-4 and HfCN-5 in Table 3).

## 4. DISCUSSION

The presence of both HfN and Hf(C, N) or Hf(O, N) phases together with the 13.1(2) wt % Hf<sub>2</sub>ON<sub>2</sub> phase in HfN-1 sample from the nitridation of HfO<sub>2</sub>-2.15C precursor at 1300 °C indicated that the nitridation of HfO<sub>2</sub> at that temperature was partial and the nitridation went through an intermediate Hf<sub>2</sub>ON<sub>2</sub> phase. Nitridation at 1400 °C in sample HfN-2 also produced two nitride phases and impurity Hf<sub>2</sub>ON<sub>2</sub> (<0.5 wt %) and  $Hf_7O_8N_4$  (<3 wt %) phases. Since a lower fraction of intermediate phases is present in the 1400 °C sample and the relative oxygen moles in  $Hf_7O_8N_4$  is greater than in  $Hf_2ON_2$ , it can be suggested that more oxygen was removed by carbon and nitrogen, resulting in higher reactivity at 1400 °C than at 1300 °C and forming more primary nitrides (HfN) in the HfN-2 sample. The presence of oxygen in the form of a Hf<sub>c</sub>O<sub>d</sub>N<sub>f</sub> type phase at a greater level in the sample synthesized at 1300 °C compared to at 1400 °C also suggests that the second HfN phase in the 1300 °C sample contains dissolved oxygen at least at a larger level than any dissolved carbon in it. The second HfN phase in the 1300 °C sample also has a refined LP of 0.45417(1) nm, which is closer to the high-end of LPs reported for Hf(O, N) phase as depicted in Figure 4. The refined LP [0.45716(1) nm] of the second phase in 1400 °C sample matches well with the reported values for Hf(C, N) type phases (Figure 4 and Table S2) confirming the presence of lower amount of oxygen in the nitride phases and in the product overall.

In the samples (HfN-3-HfN-7) synthesized at 1500-1700 °C temperatures under N<sub>2</sub> using the same HfO<sub>2</sub>-2.15C

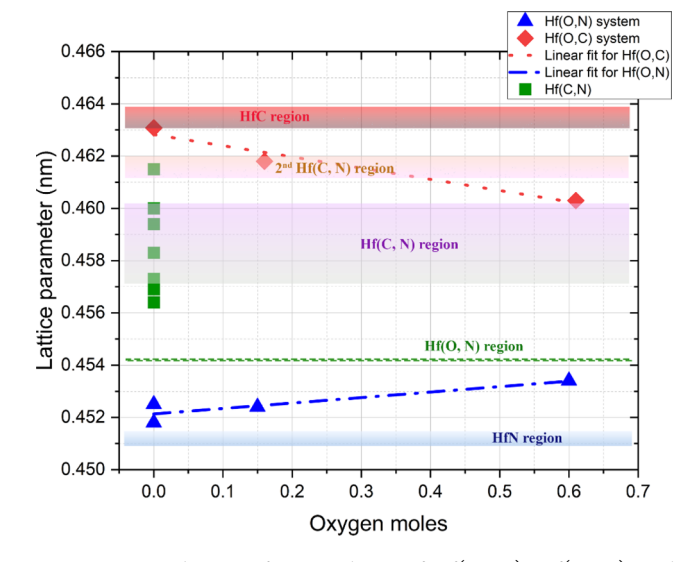


**Figure 4.** Distribution of reported LPs of Hf(O, N), Hf(O, C), and Hf(C, N) systems. The HfN, Hf(O, N), Hf(C, N), a 2nd Hf(C, N), and HfC regions of the data from the current work are highlighted by color-coded regions of blue, green, pink, orange, and red, respectively.

precursor, only Hf(C, N) phase present according to the refined LPs of the nitride phase (pink color region in Figure 4). The refined LP of Hf(C, N) phase increased with the increase in the sample synthesis temperature up to 1650 °C after which it plateaued as shown in Figure 5. This increase in LP against the synthesis temperature that plateaus at 1650 °C indicates an increase in carbon dissolution in the HfN lattice up to a maximum carbon content at that temperature for the HfO<sub>2</sub>-2.15C precursor under N<sub>2</sub> with a 24 h maximum reaction time. This observation is discussed further below.

The above results can be used to elucidate the formation of product phases for the direct nitridation reaction of HfO<sub>2</sub>-2.15C precursor using the following reaction pathways

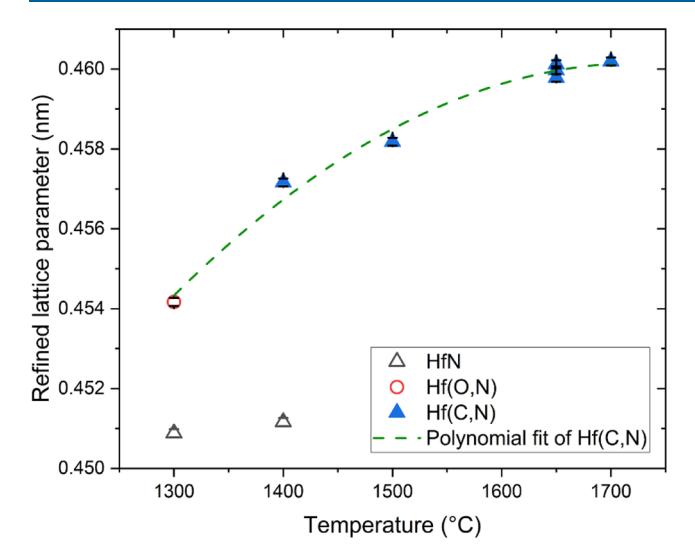


Figure 5. Refined LPs of different phases in the samples synthesized using  $HfO_2$ -2.15C precursor at different temperatures for 12 h under  $N_2$  cover gas.

$$7HfO_2 + 6C + 2N_2 \rightarrow Hf_7O_8N_4 + 6CO_{(g)}$$
 (4)

$$2Hf_7O_8N_4 + 9C + 3N_2 \rightarrow 7Hf_2ON_2 + 9CO_{(g)}$$
 (5)

$$Hf_7O_8N_4 + (8 - x)C + (3 - x)/2N_{2(g)}$$
  
 $\rightarrow 6HfN + HfN_{1-x}O_x + (8 - x)CO_{(g)}$  (6)

$$HfN_{1-x}O_x + (x + y)C + (x - y)/2N_{2(g)}$$
  
 $\rightarrow HfN_{1-y}C_y + xCO_{(g)}$  (7)

The lower amount of HfN phase fraction in the 1300  $^{\circ}$ C sample (HfN-1) compared to the 1400  $^{\circ}$ C sample (HfN-2) and the corresponding greater microstrain (Figure 6a) and smaller crystallite size (Figure 6b) of the HfN phase in the 1400  $^{\circ}$ C sample indicate that phase-pure binary HfN phase formation via direct nitridation of the HfO<sub>2</sub>-2.15C precursor is unfavorable at higher temperatures under the experimental

conditions tested, especially in the presence of carbon. The decrease in the microstrain and the increase in the crystallite size of the second phase, Hf(C, N), with the increase in temperature from 1300 to 1400 °C on the other hand indicate that the experimental conditions are favorable for the formation of that phase. Microstrain and crystallite size further showed decreasing and increasing trends with the increase in reaction temperature up to 1650-1700 °C, indicating that the Hf(C, N) phase formation is inevitable under these experimental conditions, especially at high temperatures.

Carbothermic reduction of HfO<sub>2</sub>-3.1C precursor samples at temperatures 1650-1750 °C produced single-phased HfC according to the XRD studies. As highlighted by the red color region in Figure 4, refined LPs [0.46318(1)-0.46368(1) nm] of the HfC phase of these samples also suggested that the HfC lattice is free from any significant amount of dissolved oxygen. Nitridation of both directly and following a carbothermic reduction of HfO<sub>2</sub>-3.1C produced HfNs with greater LPs than that of HfN phase and smaller LPs of HfCs, implying the presence of dissolved carbon in the nitride phase and therefore a chemical composition of  $HfC_{1-\nu}N_{\nu}$ . Profile fits of the XRD patterns using Rietveld refinement of the samples synthesized using two-step (i.e., carbothermic reduction followed by nitridation) process showed the presence of two phases. The second phase had a greater LP than the first primary phase and those values coincided with the reported LPs of both Hf(C, N)and Hf(O, C) phases (Tables S3 and S4) as depicted by the orange color region in Figure 4. However, since the carbothermic reduction of HfO2-3.1C precursor samples produced HfC with the absence of significant amount of oxygen, these second phases were identified as Hf(C, N) with more dissolved carbon resulting a general chemical phase of  $HfC_{1-y'}N_{y'}$ , where y' < y in  $HfC_{1-y}N_y$ . The level of carbon was estimated to be 0.60-0.72 and 0.75-0.80 for  $HfC_{1-y}N_y$  and  $HfC_{1-\nu'}N_{\nu'}$ , respectively, using a linear correlation plot of LP versus carbon content in Hf(C, N) from the data reported by Pialoux et al. (Figure 7 and Table S3).<sup>23</sup>

Using the same linear regression, carbon level of 0.02-0.64 was estimated for the Hf(C, N) synthesized by direct nitridation reaction of HfO<sub>2</sub>-2.15C precursor. As depicted in Figure 7, the low carbon (C/HfO<sub>2</sub> molar ratio of 2.15)

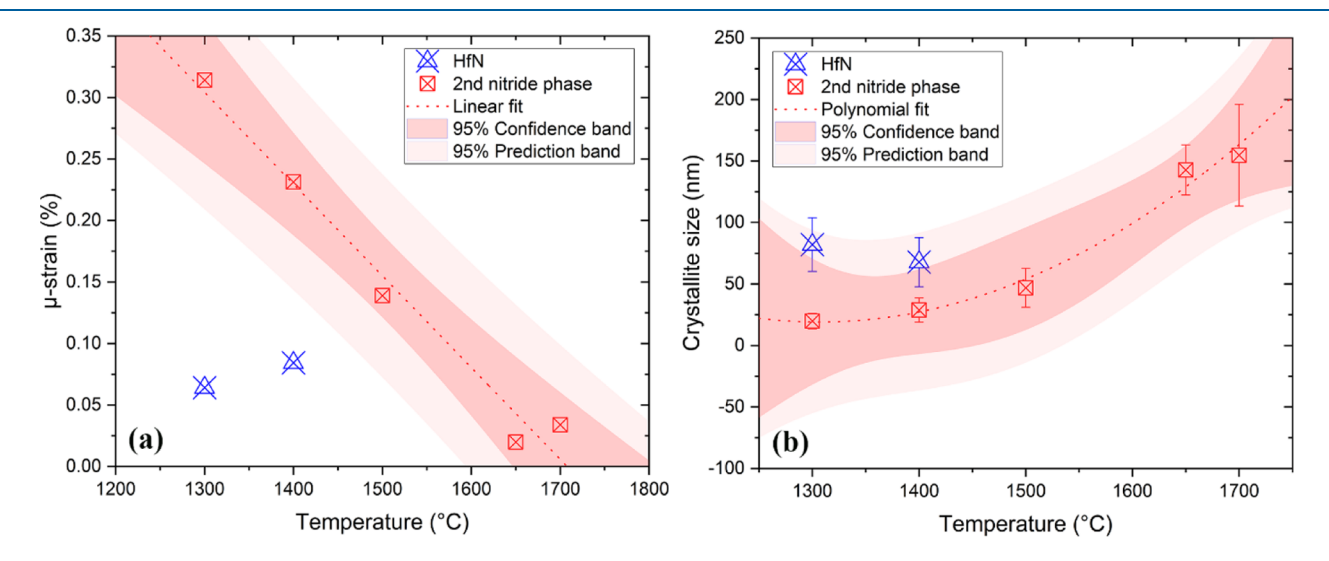
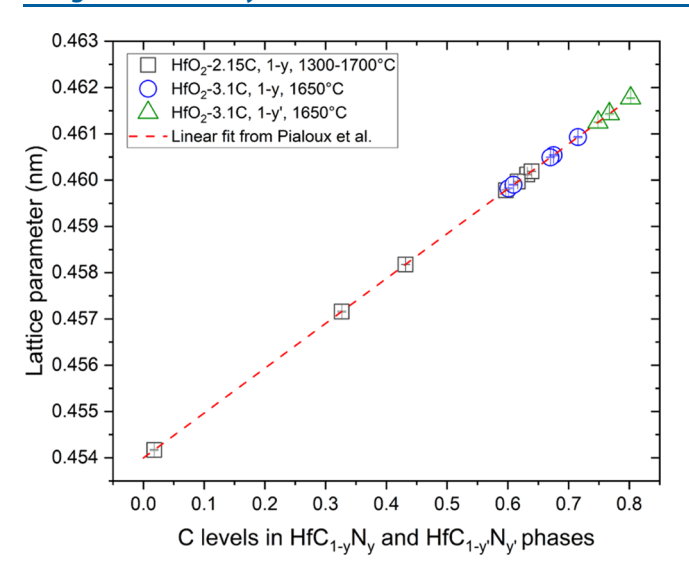


Figure 6. Variation of (a) microstrain and (b) crystallite size of product phases obtained from the nitridation of HfO<sub>2</sub>-2.15C precursor at different temperatures under  $N_{2(g)}$ .



**Figure** 7. Variation of carbon content in the Hf(C, N) samples synthesized in this study. Carbon levels were estimated using the linear regression of the data reported by Pialoux et al. <sup>23</sup> Figure depicts data correspond to (1-y) in HfC<sub>1-y</sub>N<sub>y</sub> of samples synthesized at 1300–1700 °C using HfO<sub>2</sub>-2.15 precursor. Data correspond to (1-y') in the second phase HfC<sub>1-y'</sub>N<sub>y'</sub> of samples synthesized at 1650 °C using the HfO<sub>2</sub>-3.1C precursor are also shown.

precursor samples produced Hf(C, N) phases with relatively low level of carbon, especially at low synthesis temperatures (1300–1500 °C), whereas the product phase carbon levels of samples synthesized at 1650–1700 °C are comparable with that of the samples synthesized using greater carbon level (C/HfO2 molar ratio of 3.1) precursors at high synthesis temperatures (1650–1700 °C). As discussed earlier, the highest carbon content was estimated in the second nitride phase (HfC1-y'Ny') identified in the samples synthesized using HfO2-3.1C precursor at 1650 °C. These results further indicate that Hf(C, N) is favorable at higher synthesis temperatures ( $\geq$ 1650 °C) and with greater precursor carbon content as is reported by another study where the Hf(C, N) stoichiometry observed to be dependent of the precursor C/Hf metal ratio.  $^{24}$ 

#### 5. CONCLUSIONS

Direct nitridation of HfO<sub>2</sub>-2.15C precursor samples with a C/ HfO<sub>2</sub> molar ratio of 2.15 produced HfN at temperatures of 1300 and 1400 °C. Rietveld refined LPs of second phases observed in these two samples indicated the presence of  $HfN_{1-x}O_x$  and  $HfC_{1-y}N_y$  in 1300 and 1400 °C samples, respectively. The presence of Hf<sub>2</sub>ON<sub>2</sub> in the sample synthesized at 1300 °C and the presence of Hf<sub>7</sub>O<sub>8</sub>N<sub>4</sub> and Hf<sub>2</sub>ON<sub>2</sub> in the 1400 °C sample also showed that the direct nitridation of HfO<sub>2</sub>-2.15C precursor occurred via Hf<sub>2</sub>ON<sub>2</sub> and Hf<sub>7</sub>O<sub>8</sub>N<sub>4</sub> intermediate phases. At 1500-1700 °C temperatures, the product phase only consisted of  $HfC_{1-\nu}N_{\nu}$ . The dissolution of carbon in the HfN lattice was further reflected by the increase in its LP as a function of sample synthesis temperature up to 1650 °C after which the LP plateaued. Lower lattice strain indicating higher lattice stability and greater crystallite size indicating greater crystallinity of  $HfC_{1-\nu}N_{\nu}$  suggest that Hf(C, N) is the preferable phase over HfN in the samples synthesized at elevated temperatures ( $\geq$ 1500 °C) using both 2.15 and 3.1 C/HfO<sub>2</sub> molar ratio precursors as was quantitatively determined using XRD.

Single-phased HfC was synthesized using carbothermic reduction of the HfO<sub>2</sub>-3.1C precursor with a C/HfO<sub>2</sub> molar ratio of 3.1 at 1650-1750 °C temperatures. The refined LPs of the carbides indicated that the carbide phase was free of any significantly dissolved oxygen, resulting in a nominal composition of HfC. Direct nitridation of the HfO<sub>2</sub>-3.1C precursor only produced the Hf(C, N) phase, while its carbothermic reduction followed by nitridation produced two Hf(C, N) phases with two different carbon levels with general chemical compositions of  $HfC_{1-y}N_y$  and  $HfC_{1-y'}N_{y'}$ , where 1-y'y and 1 - y' were estimated to lie in 0.60-0.72 and 0.75-0.80ranges, respectively. These results also indicate that carbothermic nitridation is a suitable synthetic route to produce  $Hf(C_i)$ N)s with chemical compositions of interest (e.g.,  $HfC_{0.75}N_{0.22}$ and  $HfC_{0.76}N_{0.24}$ ) for further characterization of their chemical and physical properties.

#### ASSOCIATED CONTENT

### Supporting Information

The Supporting Information is available free of charge at https://pubs.acs.org/doi/10.1021/acs.inorgchem.3c01333.

Rietveld analysis of the XRD pattern of the HfC sample synthesized at 1650  $^{\circ}$ C for 4 h under flowing Ar, reported HfC LPs against C/Hf molar ratio and its linear fit, comparison of profile fits of XRD patterns of HfCN-1 and HfCN-2 samples in their full and 55–73 $^{\circ}$ 2Theta ranges, Rietveld fits of the XRD patterns of the HfCN-3 sample, reported LPs for HfN and Hf(O, N) phases in the ICSD, reported LPs of the Hf(C, N) phase in the ICSD database, LP versus carbon content in Hf(C, N) reported in Pialoux et al., and reported LPs for HfC and Hf(O, C) phases in the ICSD database (PDF)

#### AUTHOR INFORMATION

#### **Corresponding Author**

Chinthaka M. Silva — Lawrence Livermore National Laboratory, Livermore, California 94550, United States; Present Address: Pacific Northwest National Laboratory, Richland, Washington 99354, United States; orcid.org/0000-0003-4637-6030; Email: chinthaka.silva@pnnl.gov

#### **Authors**

Kyle J. Kondrat – Lawrence Livermore National Laboratory, Livermore, California 94550, United States; Department of Materials Science and Engineering, University of California, Davis, California 95616, United States

Kiel S. Holliday – Lawrence Livermore National Laboratory, Livermore, California 94550, United States

Scott J. McCormack — Department of Materials Science and Engineering, University of California, Davis, California 95616, United States; orcid.org/0000-0002-0715-3451

Complete contact information is available at: https://pubs.acs.org/10.1021/acs.inorgchem.3c01333

#### **Author Contributions**

C.M.S.: methodology, formal analysis, investigation, and writing of the original draft. K.J.K.: research concept and investigation. K.S.H. and S.J.M.: research concept and funding acquisition. All authors: writing, review, and editing of the manuscript.

#### Notes

The authors declare no competing financial interest.

All data generated or analyzed during this study are included in this published article (and its Supporting Information files).

#### ACKNOWLEDGMENTS

This research was performed under the auspices of the U.S. Department of Energy (DOE) by Lawrence Livermore National Laboratory (LLNL) under contract no. DE-AC52-07NA27344. Authors also acknowledge support from the National Science Foundation (NSF), Division of Materials Research (DMR), Ceramic (CER) program under grant DMR 2047084. Authors furthermore extend their special thanks to J.L., K.H., T.L., M.G., M.K., B.C., A.S., and all my colleagues at LLNL for their support in completing this work. This manuscript has been authored by the Lawrence Livermore National Laboratory (LLNL) under contract DE-AC52-07NA27344 with the US Department of Energy (DOE). The US government retains and the publisher, by accepting the article for publication, acknowledges that the US government retains a nonexclusive, paid-up, irrevocable, worldwide license to publish or reproduce the published form of this manuscript, or allow others to do so, for US government purposes. DOE will provide public access to these results of federally sponsored research in accordance with the DOE Public Access Plan (http://energy.gov/downloads/doe-public-access-plan).

#### REFERENCES

- (1) Wittmer, M. Properties and microelectronic applications of thin films of refractory metal nitrides. *J. Vac. Sci. Technol. A* **1985**, 3, 1797—1803
- (2) Toth, L. E. Transition Metal Carbides and Nitrides; Academic Press: New York-London, 1971.
- (3) Tiwari, A.; Talwekar, R. H.; Verma, M. L. First-principles study on the structural, electronic, optical, mechanical, and adsorption properties of cubical transition metal nitrides MN (M = Ti, Zr, and Hf). *J. Electron. Mater.* **2021**, *50*, 3312–3325.
- (4) Hu, C.; Guo, K.; Li, Y.; Gu, Z.; Quan, J.; Zhang, S.; Zheng, W. Optical coatings of durability based on transition metal nitrides. *Thin Solid Films* **2019**, *688*, 137339.
- (5) Das, P.; Biswas, B.; Maurya, K. C.; Garbrecht, M.; Saha, B. Refractory plasmonic hafnium nitride and zirconium nitride thin films as alternatives to silver for solar mirror applications. *ACS Appl. Mater. Interfaces* **2022**, *14*, 46708–46715.
- (6) Escobar, C. A.; Caicedo, J. C.; Aperador, W. Corrosion resistant surface for vanadium nitride and hafnium nitride layers as function of grain size. *J. Phys. Chem. Solids.* **2014**, *75*, 23–30.
- (7) Pierson, H. O. Handbook of refractory carbides and nitrides: Properties, characteristics, processing, and applications. *Handbook of Refractory Carbides and Nitrides*; William Andrew Publishing Westwood, 1996; pp 55–80.
- (8) Roberts, B. W. Survey of superconductive materials and critical evaluation of selected properties. *J. Phys. Chem. Ref. Data* **1976**, *5*, 581–822.
- (9) Pessall, N.; Hulm, J. K. Superconducting alloys of interstitial compounds. *Physics* **1966**, *2*, 311–328.
- (10) Yamanaka, S.; Hotehama, K.; Kawaji, H. Superconductivity at 25.5 K in electron-doped layered hafnium nitride. *Nature* **1998**, 392, 580–582.
- (11) Nimmagadda, R.; Bunshah, R. F. High rate deposition of hafnium nitride by activated reactive evaporation (ARE). *Thin Solid Films* **1979**, *63*, 327–331.
- (12) Lengauer, W. Handbook of Ceramic Hard Materials; Riedel, R., Ed.; Wiley-VCH: Weinheim, 2000, pp 202–252.
- (13) O'Neill, D. B.; Frehan, S. K.; Zhu, K.; Zoethout, E.; Mul, G.; Garnett, E. C.; Huijser, A.; Askes, S. H. C. Ultrafast photoinduced heat generation by plasmonic HfN nanoparticles. *Adv. Optical Mater.* **2021**, *9*, 2100510.

- (14) Auner, G.; Padmanabhan, K. R. Effect of ion bombardment on thin hafnium nitride films. *Thin Solid Films* **1985**, *123*, 315–323.
- (15) Yu, H. Y.; Lim, H. F.; Chen, J. H.; Li, M. F.; Zhu, C.; Tung, C. H.; Du, A. Y.; Wang, W. D.; Chi, D. Z.; Kwong, D.-L. Physical and electrical characteristics of HfN gate electrode for advanced MOS devices. *IEEE Electr. Device L.* **2003**, 24, 230–232.
- (16) Wang, W.; Nabatame, T.; Shimogaki, Y. Preparation of conductive HfN by post rapid thermal annealing-assisted MOCVD and its application to metal gate electrode. *Microelectron. Eng.* **2008**, 85, 320–326.
- (17) Piedrahita, W. F.; Aperador, W.; Caicedo, J. C.; Prieto, P. Evolution of physical properties in hafnium carbonitride thin films. *J. Alloy. Compd.* **2017**, *690*, 485–496.
- (18) Hong, Q.-J.; van de Walle, A. Prediction of the material with highest known melting point from ab initio molecular dynamics calculations. *Phys. Rev. B: Condens. Matter Mater. Phys.* **2015**, 92, 020104.
- (19) Ushakov, S. V.; Navrotsky, A.; Hong, Qi-J.; van de Walle, A. Carbides and nitrides of zirconium and hafnium. *Materials* **2019**, *12*, 2728
- (20) Peng, Z.; Sun, W.; Xiong, X.; Xu, Y.; Zhou, Z.; Zhan, Z.; Zhang, H.; Zeng, Y. Novel nitrogen-doped hafnium carbides for advanced ablation resistance up to 3273K. *Corros. Sci.* **2021**, *189*, 109623.
- (21) Edwards, R. K.; Malloy, G. T. The rate of reaction of nitrogen with hafnium metal. *J. Phys. Chem.* **1958**, *62*, 45–47.
- (22) Heestand, R. L. Synthesis and fabrication of high purity hafnium nitride and hafnium carbide. *J. Vac. Sci. Technol.* **1972**, *9*, 1365–1367.
- (23) Pialoux, A. Study of the carbothermic nitriding of hafnium dioxide by high temperature X-ray diffraction. *J. Nucl. Mater.* **1993**, 200, 1–10.
- (24) Córdoba, J. M.; Sayagués, M. J.; Alcalá, M. D.; Gotor, F. J. Monophasic nanostructured powders of niobium, tantalum, and hafnium carbonitrides synthesized by a mechanically induced self-propagating reaction. *J. Am. Cer. Soc.* **2007**, *90*, 381–387.
- (25) Nepapushev, A. A.; Buinevich, V. S.; Gallington, L. C.; Pauls, J. M.; Orlova, T.; Miloserdova, O. M.; Chapysheva, N. V.; Rogachev, A. S.; Mukasyan, A. S. Kinetics and mechanism of mechanochemical synthesis of hafnium nitride ceramics in a planetary ball mill. *Ceram. Int.* 2019, 45, 24818–24826.
- (26) Zavjalov, A. P.; Nikiforov, P. A.; Kosyanov, D. Y.; Zakharenko, A. M.; Trukhin, V. O.; Talskikh, K. Y.; Shichalin, O. O.; Papynov, E. K. Phase formation and densification peculiarities of Hf-C-N solid solution ceramics during reactive spark plasma sintering. *Adv. Eng. Mater.* **2020**, *22*, 2000482.
- (27) Lyutaya, M. D.; Kulik, O. P.; Timofeeva, I. I. Kinetics of hafnium nitride formation in nitrogen and ammonia streams. *Sov. Powder Metall. Met. Ceram.* **1974**, *13*, 695–698.
- (28) Barraud, E.; Bégin-Colin, S.; Le Caër, G.; Barres, O.; Villieras, F. Mechanically activated solid-state synthesis of hafnium carbide and hafnium nitride nanoparticles. *J. alloy. Compd.* **2008**, *456*, 224–233.
- (29) Wu, Z. Y.; Chen, Z.; Wang, L.; Fang, L.; Zhou, T.; Mei, T.; Zhang, C.; Li, Q. Solid-sate synthesis of zirconium nitride and hafnium nitride powders. *J. Ceram. Soc. JPN.* **2021**, *129*, 200–203.
- (30) Peters, A. B.; Wang, C.; Zhang, D.; Hernandez, A.; Nagle, D. C.; Mueller, T.; Spicer, J. B. Reactive laser synthesis of ultra-high temperature ceramics HfC, ZrC, TiC, HfN, ZrN, and TiN for additive manufacturing. *Ceram. Int.* **2023**, *49*, 11204–11229.
- (31) Yuan, L.; Fang, G.; Li, C.; Wang, M.; Liu, N.; Ai, L.; Cheng, Y.; Gao, H.; Zhao, X. Influence of N<sub>2</sub> flow ratio on the properties of hafnium nitride thin films prepared by DC magnetron sputtering. *Appl. Surf. Sci.* **2007**, 253, 8538–8542.
- (32) Arranz, A. Synthesis of hafnium nitride films by 0.5 5 keV nitrogen implantation of metallic Hf: An X-ray photoelectron spectroscopy and factor analysis study. *Surf. Sci.* **2004**, *563*, 1–12.
- (33) Chen, Y.; Laha, T.; Balani, K.; Agarwal, A. Nanomechanical properties of hafnium nitride coating. *Scripta Mater* **2008**, *58*, 1121–1124.

- (34) Sacks, M. D.; Wang, C.-A.; Yang, Z.; Jain, A. Carbothermic reduction synthesis of nanocrystalline zirconium carbide and hafnium carbide powders using solution-derived precursors. *J. Mater. Sci.* **2004**, 39, 6057–6066.
- (35) Larson, A. C.; Von Dreele, R. B. General Structure Analysis System (GSAS); Los Alamos National Laboratory Report LAUR, 2000, pp 86–748.
- (36) Clarke, S. J.; Michie, C. W.; Rosseinsky, M. J. Structure of Zr<sub>2</sub>ON<sub>2</sub> by neutron powder diffraction: the absence of nitride-oxide ordering. *J. Solid State Chem.* **1999**, *146*, 399–405.
- (37) Bredow, T.; Lerch, M. On the anion distribution in  $Zr_7O_8N_4$ . Z. Anorg. Allg. Chem. 2007, 633, 2598–2602.
- (38) Nakamura, K.; Yashima, M. Crystal structure of (NaCl)-type transition metal monocarbides MC (M =V, Ti, Nb, Ta, Hf, Zr), a neutron powder diffraction study. *Mater. Sci. Eng. B-Adv.* **2008**, *148*, 69–72.
- (39) Bittner, H.; Goretzki, H. Magnetische Untersuchungen der Carbide Ti C, Zr C, Hf C, V C, Nb C und Ta C. *Monatsh. Chem.* **1962**, 93, 1000–1004.
- (40) Samsonow, G. W.; Morosow, W. W. Carbohydride der Uebergangsmetalle. *Monatsh. Chem.* **1971**, *102*, 1667–1678.
- (41) Samsonov, G. V.; Timofeeva, I. I. X-ray diffraction study of dynamic characteristics of crystal lattices of some interstitial phases. *Dop. Akad. Nauk. Ukrain* **1970**, 1970, 831–833.
- (42) Constant, K.; Kieffer, R.; Ettmayer, P. Ueber das pseudoternaere System HfO HfN HfC. Monatsh. Chem. 1975, 106, 973-981.
- (43) Passerini, L. Isomorfismo tra ossidi di metalli tetravalenti: I sistemi: CeO<sub>2</sub>-ThO<sub>2</sub>; CeO<sub>2</sub>-ZrO<sub>2</sub>; CeO<sub>2</sub>-HfO<sub>2</sub>. *Gzz. Chim. Ital.* **1930**, 60, 762–776.